AIAA JOURNAL
Vol. 40, No. 4, April 2002

Dynamic One-Equation Nonviscosity Large-Eddy Simulation Model

Eric Pomraning* and Christopher J. Rutland†
University of Wisconsin, Madison, Wisconsin 53706

A new approach for a nonviscosity large-eddy simulation (LES) subgrid stress model is presented. The approach uses a scaling that is provided by the subgrid kinetic energy and a tensor coefficient that is obtained from the dynamic modeling approach, hence, a dynamic structure model. Mathematical and conceptual issues motivating the development of this new model are explored. Attention is focused on dynamic modeling approaches. The basic equations that originate in dynamic modeling approaches are Fredholm integral equations of the second kind. These equations have solvability requirements that have not been previously addressed in the context of LES models. These conditions are examined for traditional dynamic Smagorinksy modeling, that is, zero-equation approaches, and one-equation subgrid models. It is shown that standard approaches do not always satisfy the integral equation solvability condition. It is also shown that traditional LES models that use the resolved scale strain rate to estimate the subgrid stresses scale poorly with filter level, leading to significant errors in the modeling of the subgrid scale stress. The poor scaling in traditional LES approaches can result in not only weak models, but can also cause nonrealizability of the subgrid stresses. A better scaling based on the subgrid kinetic energy is proposed that leads to a new one-equation nonviscosity model that does satisfy the solvability conditions and appears to maintain realizability. Both integral and algebraic formulations of the new one-equation nonviscosity model are presented. The resolved and subgrid kinetic energies are shown to compare well to a direct numerical simulation of decaying isotropic turbulence.

Nomenclature

$\boldsymbol{A}$	=	characteristic matrix
C_k	=	one-equation model viscosity coefficient
C_s	=	Smagorinsky model coefficient
C_ε	=	one-equation model dissipation coefficient
C_1	=	one-equation model coefficient at the first filter level
C_{1s}	=	Smagorinsky model coefficient at the first filter level
C_2	=	one-equation model coefficient at the test filter level
C_{2s}	=	Smagorinsky model coefficient at the test filter level
c_{ij}	=	tensor coefficient in the dynamic structure model
D	=	one-equation model diffusion coefficient
$\boldsymbol{F}$	=	vector
f	=	absolute term in a Fredholm integral equation
G	=	filter function
$\boldsymbol{G}$	=	vector
$\boldsymbol{I}$	=	identity matrix
K	=	subgrid kinetic energy at the test filter level
k	=	subgrid kinetic energy at the first filter level
L_{ij}	=	Leonard stress tensor
L_ε	=	Leonard dissipation term
P	=	pressure
S_{ij}	=	strain rate tensor
T_{ij}	=	subgrid stress tensor at the test filter level
u_i	=	velocity vector
α	=	square of length scale in infinite series expansion
α_{ij}	=	model for subgrid stress tensor at the test filter level
β_{ij}	=	model for subgrid stress tensor at the first filter level
Δ	=	filter width at first filter level
Δ_2	=	filter width at second filter level
$\tilde{\Delta}$	=	filter width at test filter level
δ	=	ratio of the second filter width to the first filter width
δ_{ij}	=	Kronecker delta
ε	=	dissipation of subgrid kinetic energy at the first filter level
ε_d	=	sink term for dissipation at the first filter level
ε_t	=	dissipation of subgrid kinetic energy at the test filter level
λ	=	parameter, eigenvalue
ν	=	kinematic viscosity
ν_t	=	Smagorinsky turbulent viscosity
ν_{tk}	=	one-equation turbulent viscosity
τ_{ij}	=	subgrid stress tensor at the first filter level
$\tau_{u_i P}$	=	unclosed term in dissipation equation
$\tau_{u_i u_i u_j}$	=	triple correlation term in subgrid kinetic energy equation
$\tau_{u_i u_k u_i}$	=	unclosed term in dissipation equation
$\tau_{u_k \varepsilon}$	=	unclosed term in dissipation equation
ϕ	=	flow variable
ψ	=	kernel of Fredholm integral equation

I. Introduction

THIS paper presents a new nonviscosity approach for modeling subgrid stresses that arise in large-eddy simulations (LES). The new approach is motivated by many difficulties with current subgrid modeling approaches. The new method takes full advantage of the powerful dynamic approach first presented by Germano et al.[1] It avoids the inaccuracies and inconsistencies inherent in relating subgrid stresses to the resolved scale strain rate tensor, which is the approach that is widely used in viscosity-based models. The dynamic structure model obtains the tensorial structure directly from the dynamic approach and uses a subgrid kinetic energy term to provide the correct scaling. The kinetic energy term is obtained from a transport equation that provides a budget between resolved and subgrid scales. The subgrid kinetic energy transport equation has two important benefits. First, it maintains numerical stability while allowing for a non-viscosity modeling approach. Second, there are strong indications that the subgrid transport equation approach works better than other approaches in engineering applications in which both the grid resolution and quality are often compromised.[2]

Received 23 February 2001; revision received 19 July 2001; accepted for publication 27 August 2001.

*Research Associate, Engine Research Center, Department of Mechanical Engineering; currently Research Engineer, Convergent Thinking, Madison, WI 53719; pomranin@c-think.com.

†Professor, Engine Research Center, Department of Mechanical Engineering.

II. LES Modeling Background

LES imply a first filter scale (or grid) that is usually chosen to be the numerical grid size. Note that the first filter is arbitrary and can be chosen to be any size desired. In fact, a first filter that is larger than the grid size may be desirable. The dynamic approach introduces another, equal, or larger test filter scale. The scaling of various common LES models at these different filter sizes becomes an important issue with significant consequences on solvability of the underlying equations and the realizability of the models. To understand these issues and, thus, the motivation for the new model, it is important to briefly review basic LES concepts.

LES is based on the decomposition of a flow variable into resolved and subgrid scale terms. The resolved terms are solved for using transport equations, whereas the subgrid terms and their effects on the resolved scales are modeled. For example, any flow variable can be decomposed as

$$\phi_i = \overline{\phi}_i + \phi_i' \tag{1}$$

where $\overline{\phi}_i$ is the filtered variable (or resolved scale) and ϕ_i' is the subgrid scale variable. The filtered variable is defined through the use of a filtering function as

$$\overline{\phi}_i(\boldsymbol{x}) = \int_V G(\boldsymbol{x}, \boldsymbol{y})\phi_i(\boldsymbol{y})\,\mathrm{d}\boldsymbol{y} \tag{2}$$

where $G(\boldsymbol{x}, \boldsymbol{y})$ is the filter function, which must satisfy

$$\int_V G(\boldsymbol{x}, \boldsymbol{y})\,\mathrm{d}\boldsymbol{y} = 1 \tag{3}$$

Typically, the filtering function is either a box or a Gaussian filter.[3] As noted earlier, the filter length is frequently chosen to be the grid size; this filter is commonly designated the grid level filter. Applying the filtering definition for a uniform nondeforming grid (here, the filter is assumed to be a function of the grid size) to the incompressible Navier–Stokes equations gives[4,5]

$$\frac{\partial \overline{u}_i}{\partial t} + \frac{\partial \overline{u}_i\,\overline{u}_j}{\partial x_j} = -\frac{\partial \bar{P}}{\partial x_i} - \frac{\partial \tau_{ij}}{\partial x_j} + \nu\frac{\partial^2 \overline{u}_i}{\partial x_j \partial x_j} \tag{4}$$

where the subgrid scale stress tensor is

$$\tau_{ij} = \overline{u_i u_j} - \overline{u}_i\,\overline{u}_j \tag{5}$$

These equations are exact; no modeling assumptions have been made at this point.[6] Note that the commonly used phrase subgrid scale stress tensor is an unfortunate choice of terminology because it is not necessarily related to the actual subgrid scale stress tensor, that is, $\tau_{ij} \neq \overline{u_i' u_j'}$ for most filters. Nevertheless, to be consistent with the literature, the term subgrid scale stress tensor should be understood to mean τ_{ij} in this paper. It is necessary to model the subgrid scale stress tensor because it cannot be readily determined from the resolved field.

Several models for the subgrid scale stress tensor have been proposed, but we believe that they are all lacking in some way. In our opinion, an ideal model should approximate the actual subgrid scale stress tensor closely. A model that fails this test does not properly capture the physical processes. It has been suggested that subgrid models only need to provide the right forcing in Eq. (4) so that the resolved scale statistics can be correctly computed.[7] However, this is a limited view, especially as LES evolves toward more complex engineering flows. In these situations, subgrid models for other terms such as scalar transport, sprays, wall functions, and combustion will be required. Having the physically correct subgrid stresses will greatly augment the modeling of these other processes just as having the turbulent kinetic energy is essential in Reynold's-averaged Navier–Stokes modeling.

Other important aspects of the ideal model are that it should properly dissipate energy from the resolved scales and allow for backscatter.[8] The model should be realizable, frame invariant, and well posed. It should not require a priori knowledge to set model constants properly. At this time, we are unaware of any models that satisfy all of these requirements. Note that the ideal model just described should not be confused with the ideal model of Langford and Moser.[9]

A. Universal Coefficient Viscosity Modeling

In general, a weakness of all LES eddy viscosity models is that the viscosity is applied over all wave numbers in the wrong proportions; additional dissipation is added where it is needed (at the higher wave numbers) and also where it is not necessary (at the lower wave numbers). Locally, energy can flow in either direction, from the subgrid scales to the resolved scales, (for example, backscatter[8]) or vice versa. A viscosity model is purely dissipative and cannot represent this process properly.

The justification for a viscosity is that it is consistent with the idea of an energy cascade, that is, the net energy flow is from larger scales to smaller scales. However, this argument may only be valid with a large sample size that might occur in ensemble- or time-averaged models. In the case of LES, where the concept of ensemble and time averaging has been removed, this argument is not valid and, therefore, the use of a viscosity energy cascade cannot be strictly justified.

The strength of viscosity models is that they often improve the numerical stability of the simulation. In addition, in an ensemble sense, they may remove the proper amount of energy from the resolved scales. However, the improved stability and proper resolved scale energy removal comes at the expense of properly representing the fluid dynamics. Thus, in general, for a viscosity model to perform well the simulation will have to be very well resolved so that the error in model will not significantly pollute the solution.

1. *Smagorinsky Model*

Probably the most commonly used subgrid scale model is the Smagorinsky viscosity model.[10] At the root of the model is the assumption that the subgrid stress tensor is a scalar multiple of the strain rate tensor. This assumption has recently been shown by Jimenez and Moser to be invalid.[11] In fact, the subgrid stress tensor correlates very poorly with the strain rate tensor as is demonstrated later in this paper. Despite this problem, the Smagorinsky subgrid scale stress tensor[10] is

$$\tau_{ij} = -2\nu_t \overline{S_{ij}} + \tfrac{1}{3}\delta_{ij}\tau_{kk} \tag{6}$$

where

$$\nu_t = C_s \Delta^2 |\bar{S}| \tag{7}$$

and the filtered strain rate tensor is defined as

$$\overline{S_{ij}} = \frac{1}{2}\left(\frac{\partial \overline{u}_i}{\partial x_j} + \frac{\partial \overline{u}_j}{\partial x_i}\right) \tag{8}$$

and the magnitude of the strain rate tensor is

$$|\bar{S}| = \left(2\overline{S_{ij}}\,\overline{S_{ij}}\right)^{\frac{1}{2}} \tag{9}$$

When the form of the model is examined, that is, a viscosity model, it is clear that energy can only flow from the resolved to the subgrid unless a negative coefficient is used. Even though the modeled subgrid stress tensor does not correlate well with the actual subgrid stress tensor, if the parameter C_s is chosen appropriately, the Smagorinsky model[10] may dissipate the correct ensemble-averaged energy from the resolved scale. However, the model may remove too much or too little energy locally even though the net energy dissipation could be correct.

An additional problem with the Smagorinsky model[10] is that it is difficult to determine the best model coefficient. It seems likely that for complex engineering flows that a single appropriate universal coefficient may not exist. In fact, for complex engineering flows, a wide range of model coefficients has been reported.[12] Modeling complex turbulent flows using the Smagorinsky model[10] requires a priori knowledge of the flow to set C_s correctly. Some of these difficulties are addressed by the dynamic Smagorinsky model[10] discussed hereafter.

2. One-Equation Eddy Viscosity Model

Recent work by others[2,13] has demonstrated that LES subgrid stress models can be improved by incorporating a transport equation for the subgrid kinetic energy. This one-equation approach may allow for coarser grids than can be used for a comparable problem with a zero-equation model because some subgrid information is available for the formulation of subgrid scale models. The exact subgrid kinetic energy equation for incompressible flow can be written as

$$\frac{\partial k}{\partial t}+\frac{\partial \overline{u_j}k}{\partial x_j}=-\overline{u_i\frac{\partial P}{\partial x_i}}+\overline{u_i}\frac{\overline{\partial P}}{\partial x_i}-\frac{\partial}{\partial x_j}\left(\frac{1}{2}\tau_{u_iu_iu_j}-\overline{u_i}\tau_{ij}\right)+\nu\frac{\partial^2 k}{\partial x_j\partial x_j}-\tau_{ij}\overline{S_{ij}}-\varepsilon \tag{10}$$

where

$$k=\tfrac{1}{2}(\overline{u_iu_i}-\overline{u_i}\,\overline{u_i}) \tag{11}$$

$$\varepsilon=\nu\left(\overline{\frac{\partial u_i}{\partial x_j}\frac{\partial u_i}{\partial x_j}}-\overline{\frac{\partial u_i}{\partial x_j}}\,\overline{\frac{\partial u_i}{\partial x_j}}\right) \tag{12}$$

$$\tau_{u_iu_iu_j}=\overline{u_iu_iu_j}-\overline{u_iu_i}\,\overline{u_j} \tag{13}$$

Again, the designation subgrid kinetic energy is a poor choice because k is not the actual subgrid kinetic energy, that is, $2k\neq\overline{u_i'u_i'}$ for most filters. Nevertheless, to be consistent with the literature,[2,13] k will be referred to as the subgrid kinetic energy in this paper. The subgrid kinetic energy equation can be modeled as

$$\frac{\partial k}{\partial t}+\frac{\partial \overline{u_j}k}{\partial x_j}=\frac{\partial}{\partial x_j}\left(D\Delta k^{\frac{1}{2}}\frac{\partial k}{\partial x_j}\right)+\nu\frac{\partial^2 k}{\partial x_j\partial x_j}-\tau_{ij}\overline{S_{ij}}-\varepsilon \tag{14}$$

where

$$\varepsilon=C_\varepsilon\left(k^{\frac{3}{2}}/\Delta\right) \tag{15}$$

$$\tau_{ij}=-2\nu_{tk}\overline{S_{ij}}+\tfrac{2}{3}k\delta_{ij} \tag{16}$$

$$\nu_{tk}=C_k k^{\frac{1}{2}}\Delta \tag{17}$$

and D, C_k, and C_ε are model coefficients.[2] Again, at the root of this model is the assumption that the subgrid stress tensor is a scalar multiple of the strain rate tensor [Eq. (16)]. Because this is not the case, the model will not accurately represent the actual subgrid stress tensor. In addition, to use this model, the user must specify appropriate universal coefficients.

B. Dynamic Modeling

Because it is difficult to set universal model coefficients without a priori knowledge, it is evident that a model that dynamically determines the coefficients from the resolved field as a function of both time and space would be better. This can be readily accomplished using the dynamic modeling approach that was proposed by Germano et al.[1] This approach is based on an assumed self-similar scaling between resolved and subgrid scales and a mathematical identity that arises. Models using the dynamic approach have become widely used. To formulate a dynamic model, a second filtering operation, which is designated the test level filter, is required. The test filter operation is defined in a similar manner as the grid filter operation except that the test level filter characteristic length $\hat{\Delta}$ is required to be equal to or larger than the grid level filter characteristic length Δ.

With the use of the definition of the test filter, a stress tensor at the test level can be defined by

$$T_{ij}=\overline{\overline{u_i}u_j}-\overline{u_i}\,\overline{u_j} \tag{18}$$

The grid level stress tensor and the test level stress tensor are related by the Germano et al. identity[1]

$$L_{ij}=T_{ij}-\bar{\tau}_{ij} \tag{19}$$

where the Leonard stress term L_{ij} is defined by

$$L_{ij}=\overline{\overline{u_i}\,\overline{u_j}}-\overline{u_i}\,\overline{u_j} \tag{20}$$

The Leonard stress term can be readily determined from the resolved velocity field in an LES simulation. Thus, Eq. (19) is extremely useful because it relates the unknown stress tensors at the two scales, τ_{ij} and T_{ij}, to a known tensor L_{ij}.

1. Dynamic Smagorinsky Model

The next step in formulating a dynamic LES subgrid model is to postulate a model for the two stress tensors. Various approaches can be taken. If it is assumed that the subgrid stress scales with the strain rate tensor, the Smagorinsky model[10] can be used. As discussed earlier, this assumption cannot be justified without resorting to ensemble averaging, which is not consistent with LES concepts. Nevertheless, using the dynamic approach with Smagorinsky models gives rise to

$$\tau_{ij}=-2C_{1s}\Delta^2|\bar{S}|\overline{S_{ij}}+\tfrac{1}{3}\delta_{ij}\tau_{kk} \tag{21}$$

$$T_{ij}=-2C_{2s}\hat{\Delta}^2\widehat{|\bar{S}|}\,\overline{S_{ij}}+\tfrac{1}{3}\delta_{ij}T_{kk} \tag{22}$$

Substituting these modeled stress tensor terms into the Germano et al.[1] identity gives the dynamic model

$$L_{ij}-\tfrac{1}{3}\delta_{ij}L_{kk}=\alpha_{ij}C_{2s}-\beta_{ij}C_{1s} \tag{23}$$

where

$$\alpha_{ij}=-2\hat{\Delta}^2\widehat{|\bar{S}|}\,\overline{S_{ij}} \tag{24}$$

$$\beta_{ij}=-2\Delta^2|\bar{S}|\overline{S_{ij}} \tag{25}$$

The dynamic Smagorinsky coefficients, C_{1s} and C_{2s}, cannot be found from Eq. (23) as formulated. Commonly, two further assumptions are made to make the model usable. First, it is assumed that the underlying Smagorinsky model scales with the filter level, and, therefore, the coefficients can be assumed equal. This scaling assumption cannot really be justified and is explored in more detail later in the paper. Second, the resulting single coefficient is assumed to vary slowly in space so that it is justifiable to move it outside of the integral. Note that this assumption cannot be justified a posteriori.[13] With these two major assumptions, Eq. (23) becomes

$$L_{ij}-\tfrac{1}{3}\delta_{ij}L_{kk}=C_sM_{ij} \tag{26}$$

where

$$M_{ij}=\alpha_{ij}-\overline{\beta}_{ij} \tag{27}$$

The problem has now been reduced to a set of nine algebraic equations (six when symmetry is considered). To reduce the problem to a single algebraic equation, Lilly[14] proposed using a least-squares technique to minimize the error resulting in the following single algebraic expression:

$$C_s=\left(\frac{L_{ij}M_{ij}}{M_{kl}M_{kl}}\right) \tag{28}$$

The dynamic coefficients obtained in this manner may be positive or negative. A positive coefficient implies that energy flows from the resolved to the subgrid scales, whereas a negative coefficient implies energy flows from the subgrid scales to the resolved scales. Whereas this backscatter behavior has a physical basis,[8] in practice, for this formulation, it can be excessive.[13] The unchecked modeled backscatter leads to numerical instability that is usually addressed with additional ad hoc averaging either in homogeneous spatial directions[1] or in time.[15] The spatial averaging becomes difficult in applications without homogeneous directions. This has severely limited the use of this model unless drastic measures are taken such as arbitrarily restricting the model coefficients in Eq. (28) to be positive. Note that even though the dynamic model allows for the modeling of backscatter, a simple negative viscosity (or coefficient) cannot accurately represent the complex phenomena of backscatter.

2. One-Equation Dynamic Model

An alternative dynamic modeling approach has been described by Ghosal et al.[13] to address the numerical instability associated with the unchecked energy flow from the subgrid to the resolved scales. A transport equation for the subgrid turbulent kinetic energy is added to the dynamic model to enforce a budget on the energy flow between the resolved and the subgrid scales. To that end, the subgrid stress tensor models are required to be a function of the subgrid turbulent kinetic energy. The one-equation model for the stress tensors are given by

$$\tau_{ij} = -2C_1 \Delta k^{\frac{1}{2}} \overline{S_{ij}} + \tfrac{2}{3}\delta_{ij} k \tag{29}$$

$$T_{ij} = -2C_2 \hat{\Delta} K^{\frac{1}{2}} \overline{S_{ij}} + \tfrac{2}{3}\delta_{ij} K \tag{30}$$

where the grid and test level turbulent kinetic energies are defined by

$$k = \tfrac{1}{2}(\overline{u_i u_i} - \overline{u_i}\,\overline{u_i}) \tag{31}$$

$$K = \tfrac{1}{2}(\overline{\overline{u_i} u_i} - \overline{u_i}\,\overline{u_i}) \tag{32}$$

The grid level subgrid scale turbulent kinetic energy is found from the transport equation given in Eq. (14), where the coefficients may be dynamically determined.[13] The test level and grid level turbulent kinetic energies are related by the trace of Leonard term so that another transport equation for K is not required:

$$K = \bar{k} + \tfrac{1}{2} L_{ii} \tag{33}$$

Again, if the model for subgrid stress tensors scales with the filter level, then the coefficients C_1 and C_2, in Eqs. (29) and (30), can be replaced by a single coefficient, C. Now, the integral equations can be written as

$$L_{ij} - \tfrac{1}{3}\delta_{ij} L_{kk} = \alpha_{ij} C - \overline{\beta_{ij}} C \tag{34}$$

where

$$\alpha_{ij} = -2\hat{\Delta} K^{\frac{1}{2}} \overline{S_{ij}} \tag{35}$$

$$\beta_{ij} = -2\Delta k^{\frac{1}{2}} \overline{S_{ij}} \tag{36}$$

Note that the coefficient C is properly left inside the integral. To solve for C, in this form, the integral equations may be recast as a variational problem to find the best fit for C. The result is a single Fredholm integral equation of the second kind, which can be solved using an iterative method.

The one-equation dynamic model of Ghosal et al.[13] was shown to compare well with direct numerical simulation (DNS) results. It addresses the problem of negative model coefficients and the inverse energy cascade by enforcing a budget on the subgrid energy. However, the solvability of the integral formulation is not addressed, and there is indication that the iterative solution for the coefficient C did not always converge. Also, the model is not strictly realizable,[13,16] as discussed hereafter. In addition, scaling issues between the two filter levels that the dynamic modeling approach depends on were not investigated.

III. Coefficient Isotropy and Scaling

The issues brought out in the models just described have prompted an examination of the assumptions and requirements of subgrid models. All of the models mentioned and most LES models currently in use relate the subgrid stress tensor to the strain rate tensor by a scalar coefficient. In other words, they assume isotropy in the coefficient. Also, in the case of most dynamic models, it is assumed that the subgrid stress model coefficients scale with filter size at both filter levels. In this section, a more thorough investigation of these modeling assumptions is made.

To investigate these assumptions, a DNS of fully developed isotropic turbulence, using a pseudospectral code,[17] with a Taylor scale Reynolds number of approximately 30, is used. The DNS used a 64^3 grid, and the results were filtered to determine the LES subgrid modeled stress tensors. A modest flowfield is chosen because of the computational expense of solving Fredholm integral equations, which is required in Sec. V. The LES grid filter length scale Δ is set to twice the DNS grid size, and the LES test filter length scale $\hat{\Delta}$ is set to four times the grid size.

The isotropic, scalar relation assumption is checked using the one-equation LES model of Ghosal et al.[13] and the nondynamic Smagorinsky model.[10] The exact subgrid turbulent kinetic energy k is determined by filtering the DNS field appropriately. The subgrid scale stress tensors are modeled by more general forms of Eq. (29) and (21), in which a full set of coefficients are retained to check the isotropic assumption. This is done strictly to evaluate the validity of the isotropic scalar relation and is not part of a proposed model. In this case, the evaluation models become

$$\tau_{ij} = -2C_{1[ij]} \Delta k^{\frac{1}{2}} \overline{S_{[ij]}} + \tfrac{2}{3}\delta_{ij} k \tag{37}$$

$$\tau_{ij} = -2C_{1[ij]} \Delta^2 |\bar{S}| \overline{S_{[ij]}} + \tfrac{1}{3}\delta_{ij} \tau_{kk} \tag{38}$$

Note that, throughout this paper, the square brackets indicate no summation on repeated indices, and this notation is only used when checking modeling assumptions. With these expressions, the six coefficients are determined by equating the exact subgrid scale stress tensor, obtained from the DNS field, to the modeled stress tensor terms. The coefficients determined in this manner at the grid level are denoted as $C^{\mathrm{DNS}}_{1[ij]}$, whereas the coefficients determined at the test level in this manner are denoted by $C^{\mathrm{DNS}}_{2[ij]}$. Note that the set of coefficients $C_{1[ij]}$ and $C_{2[ij]}$ do not form a tensor; they are simply a set of coefficients used for checking the coefficient isotropy and scaling. Thus, the analysis that follows is only correct for the frame of reference considered for this test. However, if a model performs poorly in any frame of reference, then the model is lacking. With the coefficients determined from DNS, a normalized variation in the coefficients at the grid level can be defined by

$$\sigma_1 = \frac{\left| C^{\mathrm{DNS}}_{1[ij]} - C^{\mathrm{DNS}}_{1[11]} \right|}{\sum_{i,j} \left| C^{\mathrm{DNS}}_{1[ij]} \right| / 9} \tag{39}$$

This expression quantifies the variation from a reference value taken as the local $C^{\mathrm{DNS}}_{1[11]}$ term. The variation is evaluated at all grid points and for all i and j terms (with the exception of $i = j = 1$) to form a probability density function (PDF) that is shown in Fig. 1. The spread in the PDF away from zero is very broad, which indicates a wide variation in the six coefficients. Because there is a wide variation in the model coefficients, the isotropic coefficient assumption is difficult to justify. At the root of the problem is the assumption that the subgrid stress tensor is related to the strain rate tensor by a scalar.

The second modeling assumption issue to address is whether the grid and test level stress tensors scale with the filter size. This is addressed in a manner similar to the first issue. This issue of scaling is central to the accuracy of any dynamic model because the Germano et al.[1] identity exactly relates the difference in the subgrid scale stress tensors at different scales to the Leonard term. Models that do not scale properly at the different filter levels will result in a poor estimation of the actual subgrid scale stress tensor. A PDF of the normalized variation in the coefficients at the two filter levels is determined using

$$\sigma_2 = \frac{\left| C^{\mathrm{DNS}}_{1[ij]} - C^{\mathrm{DNS}}_{2[ij]} \right|}{\left| C^{\mathrm{DNS}}_{1[ij]} \right|} \tag{40}$$

The result of evaluating this variation over the entire domain and for all indices is shown in Fig. 2. This shows that there is a wide variation in the stress tensor coefficients at the two different filter levels. Thus, for this case, the modeled terms do not scale well with the different filter levels. Because of the poor scaling, the dynamic modeling approach will suffer, and a model that scales well with different filter levels should be formulated.

Note that both of the tests for isotropy and scaling were only performed at relatively low Reynolds number (based on the grid

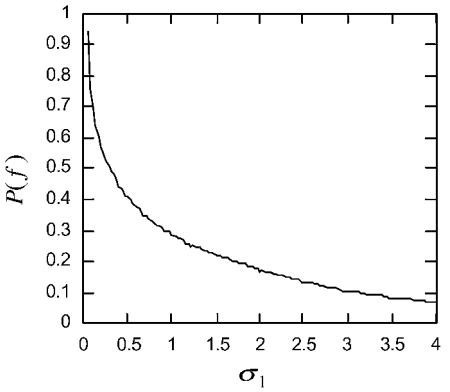

One-equation dynamic model, Eq. (29)

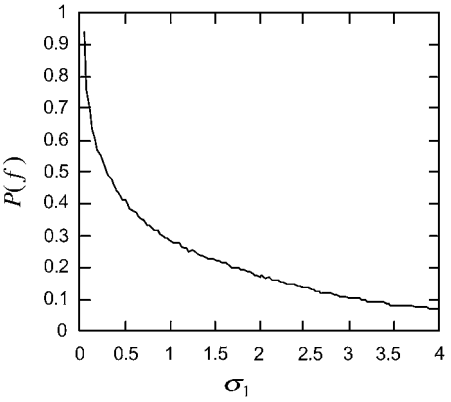

Smagorinsky model,[10] Eq. (7)

Fig. 1 PDFs indicating the variation of the model coefficients from isotropy, where σ_1 is defined in Eq. (39) and values of zero indicate isotropy.

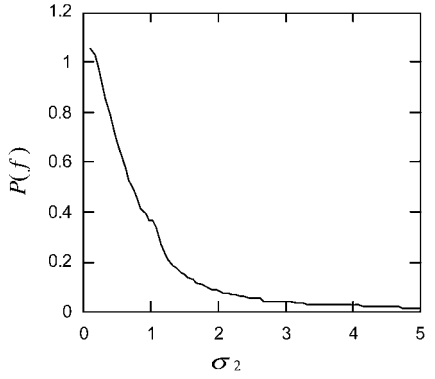

One-equation dynamic model, Eq. (29)

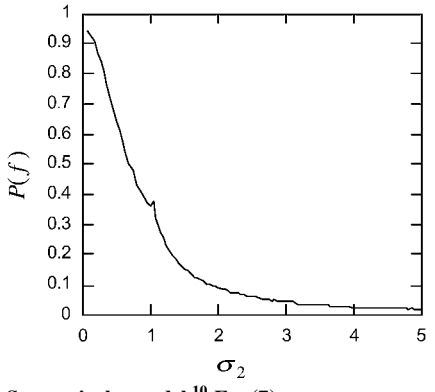

Smagorinsky model,[10] Eq. (7)

Fig. 2 PDFs showing the poor scaling of model coefficients at different filter sizes, where σ_2 is defined in Eq. (40) and values near zero indicate good scaling.

resolution). Because the simulations were run at low Reynolds numbers, it may not be appropriate to conclude that the same difficulties would occur at higher Reynolds numbers. However, it would seem reasonable to insist that the models perform well at low Reynolds numbers and, therefore, that the models that do not perform well should be improved.

IV. Solvability of the Dynamic Model

Integral equations are fundamental to the dynamic modeling approach and occur naturally when stress tensor models are placed into the Germano et al.[1] identity. However, only under certain conditions can the Fredholm integral equations be solved. Even approaches that avoid the integral equations, for example, the minimization technique of Lilly,[14] should consider the solvability conditions of the underlying equations from which their models are derived. Without a proper foundation, it is reasonable to expect that difficulties or inconsistencies could arise.

The general form of a Fredholm integral equation of the second kind can be written as

$$g(\boldsymbol{x}) = f(\boldsymbol{x}) + \lambda \int_a^b \psi(\boldsymbol{x}, \boldsymbol{y}) g(\boldsymbol{y})\, \mathrm{d}\boldsymbol{y} \tag{41}$$

where f is the absolute term, λ is a parameter, and ψ is the kernel.[18] The theorem that governs the solvability of Fredholm integral equations is known as the Fredholm alternative.[18] Briefly, the theorem states that a unique solution exists if λ is not an eigenvalue of the associated homogeneous problem

$$g(\boldsymbol{x}) - \lambda \int_a^b \psi(\boldsymbol{x}, \boldsymbol{y}) g(\boldsymbol{y})\, \mathrm{d}\boldsymbol{y} = 0 \tag{42}$$

In typical LES simulations, the underlying equations do not lend themselves well to using this theorem for examining the solvability of the model. Fortunately, an analogous theorem can be shown for the finite difference approximations to the equations.

Typically, in LES applications the governing equations are approximated using finite differences. In these applications, the integral equations can be replaced by finite difference approximations.[19] If the integral is replaced by a discrete sum, Eq. (41) can be written as

$$g(\boldsymbol{x}) - \lambda \sum_{j=1}^{n} \frac{1}{n} \psi\left(\boldsymbol{x}, \frac{j}{n}\right) g\left(\frac{j}{n}\right) = f(\boldsymbol{x}) \tag{43}$$

Now, if the sum is evaluated only n times at i discrete locations, then the sum can be written as

$$g\left(\frac{i}{n}\right) - \lambda \sum_{j=1}^{n} \frac{1}{n} \psi\left(\frac{i}{n}, \frac{j}{n}\right) g\left(\frac{j}{n}\right) = f\left(\frac{i}{n}\right), \qquad i = 1, 2, \ldots, n \tag{44}$$

Rewriting this equation in matrix form gives

$$(\boldsymbol{I} - \lambda \boldsymbol{A})\boldsymbol{G} = \boldsymbol{F} \tag{45}$$

and solving for the vector $\boldsymbol{G}$ gives

$$\boldsymbol{G} = (\boldsymbol{I} - \lambda \boldsymbol{A})^{-1} \boldsymbol{F} \tag{46}$$

Thus, a solution to this discretized Fredholm integral equation exists provided λ is not a root (or eigenvalue) of the expression

$$\det(\boldsymbol{I} - \lambda \boldsymbol{A}) = 0 \tag{47}$$

Equation (47) is used to evaluate the solvability of dynamic LES models.

To evaluate traditional dynamic models in which the coefficient is left inside of the integral, for example, Eq. (34), a minimization procedure is required to reduce the number of integral equations to the number of unknowns. Ghosal et al.[13] developed a procedure to minimize the dynamic coefficient while properly leaving it inside of the integral. For comparison and completeness, the outcome of this

minimization procedure is shown here. The result of their procedure is a Fredholm integral equation of the second kind written here as

$$C(\boldsymbol{x}) = f(\boldsymbol{x}) + \lambda \int_V \psi(\boldsymbol{x},\boldsymbol{y}) C(\boldsymbol{y})\, \mathrm{d}\boldsymbol{y} \tag{48}$$

where C is the dynamically determined coefficient with

$$\psi(\boldsymbol{x},\boldsymbol{y}) = \left(\frac{\alpha_{ij}(\boldsymbol{x})\beta_{ij}(\boldsymbol{y})}{\alpha_{mn}(\boldsymbol{x})\alpha_{mn}(\boldsymbol{x})} + \frac{\alpha_{ij}(\boldsymbol{y})\beta_{ij}(\boldsymbol{x})}{\alpha_{mn}(\boldsymbol{x})\alpha_{mn}(\boldsymbol{x})} - \frac{\int_V \beta_{ij}(\boldsymbol{x})\beta_{ij}(\boldsymbol{z}) C(\boldsymbol{z}) G(\boldsymbol{y},\boldsymbol{z})}{\alpha_{mn}(\boldsymbol{x})\alpha_{mn}(\boldsymbol{x})} \right) G(\boldsymbol{x},\boldsymbol{y}) \tag{49}$$

$$f(\boldsymbol{x}) = \frac{L_{ij}(\boldsymbol{x})\alpha_{ij}(\boldsymbol{x})}{\alpha_{mn}(\boldsymbol{x})\alpha_{mn}(\boldsymbol{x})} - \frac{\beta_{ij}(\boldsymbol{x})\overline{L_{ij}}(\boldsymbol{y})}{\alpha_{mn}(\boldsymbol{x})\alpha_{mn}(\boldsymbol{x})} \tag{50}$$

and $\lambda = 1$.

As shown, if the resulting integral equation is discretized, the roots of the characteristic matrix can be determined. If λ is a root (or eigenvalue) of the characteristic matrix, then the Fredholm integral equation is not solvable. This verification was made for both the dynamic Smagorinsky model (see Ref. 1) and the dynamic one-equation model of Ghosal et al.[13] A modest 16^3 isotropic turbulent field was used for this analysis (4096 eigenvalues) because of the computational expense associated with calculating the roots of the matrix. However, regardless of the field size, if it is found that the corresponding integral equations are unsolvable, then the model has been shown to be lacking. Figure 3 shows the PDF of the reciprocal eigenvalues ($1/\lambda$) for the characteristic matrix. As can be seen, the spectrum of eigenvalues spans unity for both models, and, therefore, there is a possibility that the model may be unsolvable. At any single time, it is unlikely that an eigenvalue of the characteristic matrix will be unity. However, when one considers that the eigenvalues are continuous in time, it is very likely that there are times when an eigenvalue of the characteristic matrix is unity, and, thus, the problem cannot be solved. Furthermore, any eigenvalue close to unity may make it difficult to find a converged numerical solution. When Fig. 3 is referred to, it is possible to determine the fraction of integral equations that will not be numerically solvable for the test case considered. Of course, for different cases the PDF of eigenvalues will be different. It may appear that the solvability is an innocuous problem, but if the integral equations are unsolvable at any time, the simulation cannot proceed with any confidence. Based on the authors' experience, solvability will be an issue for the integral equations on a regular basis.

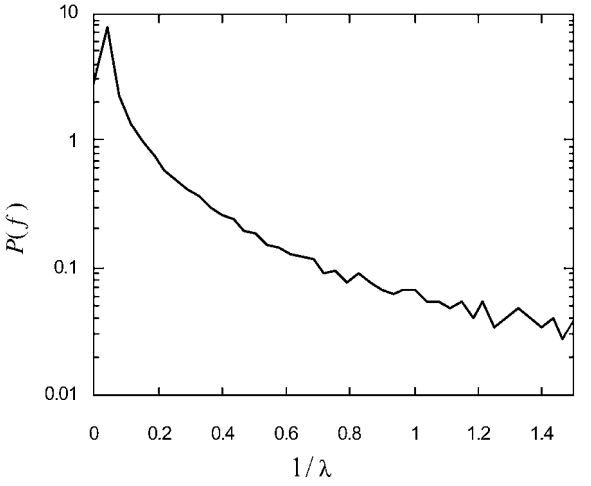

Dynamic Smagorinsky model (see Ref. 1)

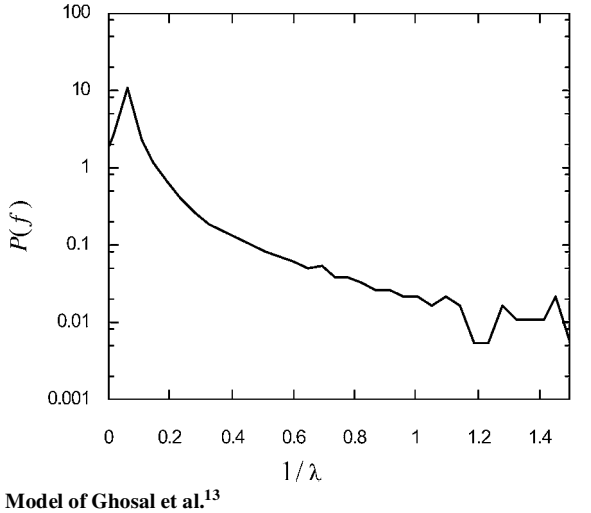

Model of Ghosal et al.[13]

Fig. 3 PDF of the reciprocal eigenvalues of the characteristic matrix. The eigenvalues span unity for which the Fredholm integral equation is unsolvable.

V. One-Equation Nonviscosity Dynamic Model

To address some of the mathematical and conceptual difficulties in the common LES models, a new one-equation nonviscosity dynamic model (dynamic structure model[20]) has been developed. Instead of modeling the stress tensor using a turbulent viscosity, an attempt is made to estimate the stress tensor directly. (Note that the reference to nonviscosity refers to the absence of a turbulent viscosity in the model; it does not mean that the molecular viscosity has been removed from the governing equations.) A transport equation for the subgrid turbulent kinetic energy is added to the dynamic model to provide scaling and enforce a budget on the energy flow between the resolved and the subgrid scales. The one-equation model for the grid and test level stress tensors are given by

$$\tau_{ij} = c_{ij} k \tag{51}$$

$$T_{ij} = c_{ij} K \tag{52}$$

This model obtains the tensor structure of the subgrid stresses from a tensor coefficient rather than from the resolved scale stress tensor. As shown hereafter, the tensor coefficient is found using the Germano et al.[1] identity. Additionally, it is reasoned that because the subgrid kinetic energy is related to the trace of the subgrid stress tensor, a model of this form will scale well at the two filter levels. For this reason, it is assumed that the tensor coefficient is the same at both filter levels. Clearly, by assuming a single tensor coefficient, we have implicitly assumed that the two subgrid stress tensors and the Leonard term are aligned. Of course, scale similarity models also make use of the alignment assumption.[21–23] The validity of this assumption is checked hereafter.

Substituting these models for the two stress tensors into the Germano et al.[1] identity gives the following:

$$L_{ij} = K c_{ij} - \overline{k c}_{ij} \tag{53}$$

Note that the coefficient tensor c_{ij} is properly left inside the integral indicated by the curved overbar. The result is a set of six (the stress tensor is symmetric) Fredholm integral equations of the second kind that can be solved using an iterative method. Alternatively, an algebraic form of the model is obtained by assuming the tensor coefficient can be removed from the integral in Eq. (53). Both the integral and algebraic form of the model are investigated hereafter.

In typical LES models, the structure of the subgrid stress tensor comes from the strain rate tensor. As discussed earlier, this modeling approach leads to poor representation of the subgrid stress tensor. For the nonviscosity model, the structure of the subgrid stress tensor comes from the Leonard term. The structure of the new model can be seen in the algebraic form where the tensor coefficient is removed from the integral in Eq. (53) (note that to justify removing the coefficient from the integral the coefficient should not be a strong function of space). The algebraic model for the subgrid stress tensor becomes

$$\tau_{ij} = L_{ij}(2k/L_{ii}) \tag{54}$$

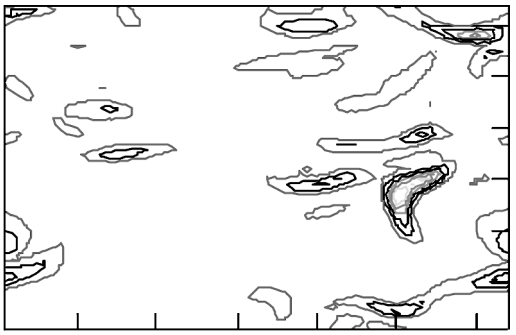

Determined from the filtered DNS field

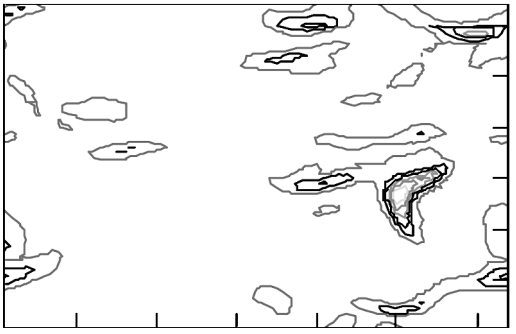

Based on the new nonviscosity model, Eq. (51)

Fig. 4 Contour plots of τ_{11}.

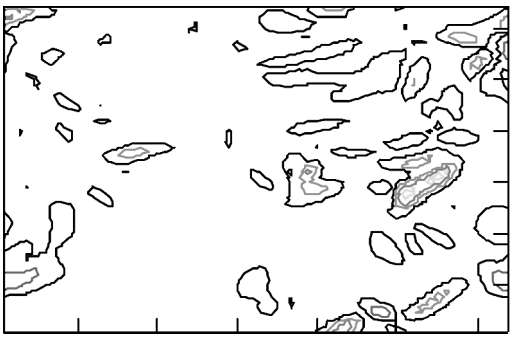

Determined from the filtered DNS field

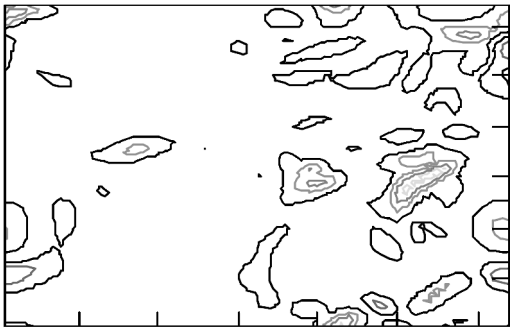

Based on the new nonviscosity model, Eq. (51)

Fig. 5 Contour plots of τ_{12}.

Thus, the new nonviscosity model scales the Leonard term by the ratio of the subgrid kinetic energy and the trace of the Leonard term. Note that the algebraic form of the model is similar in form to scale similarity models and similar to a zero-equation dynamic model proposed by Liu et al.[23] The advantage of the current approach is that the Leonard term is rescaled with the subgrid kinetic energy k, and the subgrid kinetic energy transport equation enforces a budget on energy. This budget removes the need for an added dissipative term commonly used in mixed models.

With the same 64^3 DNS simulation of decaying isotropic turbulence described earlier in this paper, the new model for the subgrid stress tensor is tested against the filtered DNS data. Again, the subgrid kinetic energy is calculated exactly from the filtered DNS field. As can be seen from Figs. 4 and 5, there is excellent agreement between the filtered DNS data and the modeled stress tensor. Note that good model correlation with the actual subgrid stress tensor does not necessarily guarantee that the model is good. More tests are required to ensure that other properties of the ideal model are met. Toward this end, solvability, scaling, invariance, and realizability of the new model are discussed in the following subsections.

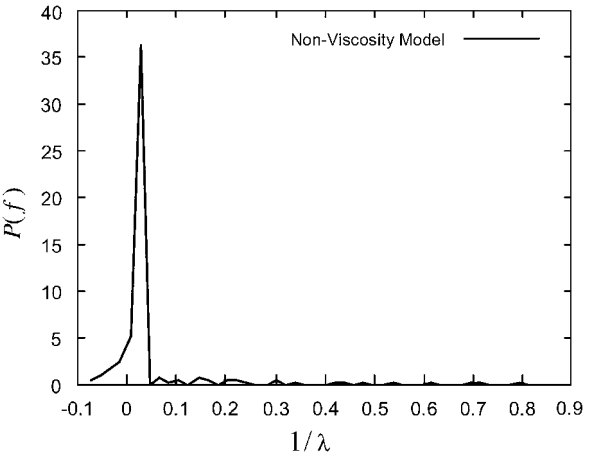

Fig. 6 PDF of eigenvalues of characteristic matrix (new one-equation model).

A. Solvability

As discussed earlier, there are restrictions on the solvability of Fredholm integral equations. The dynamic Smagorinsky model (see Ref. 1) and the dynamic one-equation model of Ghosal et al.[13] in general do not meet the solvability requirements. However, the new one-equation model does meet the solvability requirements. A check of the solvability for the new model is made by determining the roots of the characteristic matrix (47). As can be seen from Fig. 6, the roots do not span unity and, therefore, the Fredholm integral equations are solvable.

B. Scaling

The scaling assumption made in the new nonviscosity model formulation is checked by comparing the scaling of the proposed new model to that of the one-equation model of Ghosal et al.[13] using the variance defined in Eq. (40). A PDF of the normalized variation in the coefficients at the two filter levels for the two different models is shown in Fig. 7. Because the values of σ_2 are closer to zero, the new model shows significantly better scaling characteristics between the filter levels. The improved scaling validates the assumption of a single tensor coefficient at both filter levels that was made in the formulation of the new model. In addition, the benefit of the improved scaling can also be seen in contour plots of the subgrid scale stress tensor (Figs. 4 and 5).

C. Frame Invariance

Because the actual subgrid stress tensor is frame invariant, it is reasonable to insist that the model for the subgrid stress tensor be frame invariant. To verify the frame invariance of the new model, it is necessary to evaluate the frame invariance of each term in the new model. It is easy to show that the Leonard term L_{ij} and the subgrid kinetic energy k or K are frame invariant.[13] Because each term in the integral equation (53) for the tensor coefficients c_{ij} is frame invariant, the tensor coefficients are frame invariant, and, thus, the one-equation nonviscosity model is frame invariant.

D. Realizability

Finally, we briefly discuss realizability of dynamic subgrid models. Schumann[16] has shown that for a subgrid scale stress tensor to

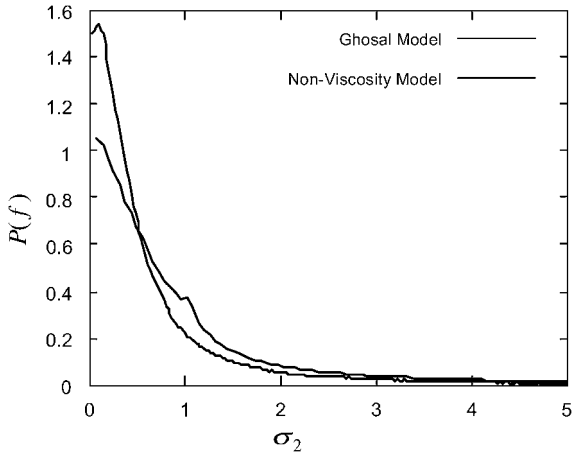

Fig. 7 PDFs showing the scaling of model coefficients at different filter sizes, where σ_2 is defined in Eq. (40) and values near zero indicate good scaling.

guarantee a realizable solution, the following conditions cannot be violated:

$$\tau_{ij} \geq 0 \qquad \text{for} \qquad i = j \tag{55}$$

$$\tau^2_{[ij]} \leq \tau_{[ii]}\tau_{[jj]} \qquad \text{for} \qquad i \neq j \tag{56}$$

$$\det(\tau_{ij}) \geq 0 \tag{57}$$

For nonnegative filters, the realizability conditions also hold for the LES subgrid stress tensor.[24]

For the DNS case considered, the nonviscosity model was found to satisfy the realizability conditions 100% of the time. Of course, this is a very limited data set and does not constitute a proof. However, based on experience and preliminary analysis, we postulate without proof that conditions for realizability of subgrid models will be related to issues of scaling and solvability of the underlying equations.

VI. Subgrid Kinetic Energy Model

The dynamic, nonviscosity based subgrid stress model just presented requires the subgrid turbulent kinetic energy. This can be obtained from a transport equation that is developed in this section. The equation introduces several additional unclosed terms that require modeling. Issues relevant to modeling these terms are explored, and appropriate models are formulated. These models should be as accurate as possible because the subgrid kinetic energy has a direct impact on subgrid models for stress and potentially scalar transport. Note that ensemble averaging is not used in LES so that resorting to statistical arguments is avoided. Also, in keeping with the nonviscosity nature of the preceding subgrid stress model, turbulent eddy viscosity ideas are not used in modeling terms of the kinetic energy equation.

To develop a modeled subgrid kinetic energy equation, we start with the exact incompressible subgrid kinetic energy equation (10). An examination of Eq. (10) reveals that there are three new terms that must be modeled: the pressure–velocity term, the triple correlation term $\tau_{u_iu_iu_j}$, and the dissipation term ε. Note that by using the Cauchy–Schwarz inequality for nonnegative filters, the subgrid kinetic energy and the dissipation term can be shown to be positive.[13]

Again, because the subgrid stress is dynamically estimated using the subgrid kinetic energy, it is critical that the unclosed terms be modeled as accurately as possible. To gain insight into the unclosed terms, it is useful to look at the infinite series expansions for each term. For a regular uniform grid ($\mathrm{d}x = \mathrm{d}y = \mathrm{d}z$) Bedford and Yeo[25] derived

$$\overline{fg} - \bar{f}\bar{g} = 2\alpha \frac{\partial \bar{f}}{\partial x_k}\frac{\partial \bar{g}}{\partial x_k} + \frac{1}{2!}(2\alpha)^2 \frac{\partial^2 \bar{f}}{\partial x_k \partial x_l}\frac{\partial^2 \bar{g}}{\partial x_k \partial x_l} + \frac{1}{3!}(2\alpha)^3 \frac{\partial^3 \bar{f}}{\partial x_k \partial x_l \partial x_m}\frac{\partial^3 \bar{g}}{\partial x_k \partial x_l \partial x_m} + \cdots \tag{58}$$

where

$$\alpha(y) = \int_{-\infty}^{\infty} x^2 G(x, y)\,\mathrm{d}x \tag{59}$$

and $G(x, y)$ is the filter function. For a box filter, it is easy to show that $\alpha = \Delta^2/24$. These series can be derived by repeated use of Taylor series expansions and a great deal of algebra. They are extremely useful because they relate an unknown term to an infinite series of known terms. Thus, they can provide important guidance in developing and evaluating models of unclosed terms. Note that Eq. (58) implies that given any resolved field, filter size, and filter shape there is only one consistent subgrid stress.

The first term that we will examine is the triple correlation term $\tau_{u_iu_iu_j}$. Using Eq. (58) and setting $f = u_iu_i$ and $g = u_j$ gives

$$\tau_{u_iu_iu_j} = 2\alpha \frac{\partial(\overline{u_i}\,\overline{u_i} + \cdots)}{\partial x_k}\frac{\partial \overline{u_j}}{\partial x_k} + \frac{1}{2!}(2\alpha)^2 \frac{\partial^2(\overline{u_i}\,\overline{u_i} + \cdots)}{\partial x_k \partial x_l}\frac{\partial^2 \overline{u_j}}{\partial x_k \partial x_l} + \cdots \tag{60}$$

Thus, we will seek a model that, when expanded as an infinite series, is similar to Eq. (60). One such model for $\tau_{u_iu_iu_j}$ is $2\overline{u_i}\,\tau_{ij}$, or, equivalently, $2(\overline{u_iu_iu_j} - \overline{u_i}\,\overline{u_i}\,\overline{u_j})$. The series expansion for this model is

$$2\overline{u_i}\,\tau_{ij} = 2\overline{u_i}\,(2\alpha)\frac{\partial \overline{u_i}}{\partial x_k}\frac{\partial \overline{u_j}}{\partial x_k} + 2\overline{u_i}\,\frac{1}{2!}(2\alpha)^2 \frac{\partial^2 \overline{u_i}}{\partial x_k \partial x_l}\frac{\partial^2 \overline{u_j}}{\partial x_k \partial x_l} + \cdots \tag{61}$$

An examination of Eqs. (60) and (61) reveals that the first terms in the series are identical. Also, the expansion shows that the leading error term is fourth order in space. Thus, this model is adopted for the triple correlation term.

An alternative approach might be to use the expanded series (60) directly. However, this approach generates more terms and requires significantly more computational effort. Furthermore, the form of the first model (61) nicely cancels with an existing term in the subgrid kinetic energy equation (10).

The second term to be modeled is the pressure–velocity term. This term may be modeled directly using Eq. (58). Setting $f = \partial P/\partial x_i$, $g = u_i$, and substituting into Eq. (58) gives

$$-\overline{u_i \frac{\partial P}{\partial x_i}} + \overline{u_i}\frac{\partial \bar{P}}{\partial x_i} = -2\alpha \frac{\partial^2 \bar{P}}{\partial x_i \partial x_k}\frac{\partial \overline{u_i}}{\partial x_k} + \cdots \tag{62}$$

If just the first term of the series is kept, the leading error term is fourth order in space. Note that as many terms as desired can be kept to make the order of accuracy of the model as high as desired. However, adding higher-order terms is computationally expensive. Also, in many cases, the pressure term effects are small relative to the production term $\tau_{ij}\overline{S_{ij}}$ and the dissipation term ε, and, therefore, the term may be neglected.

The last term that needs to be modeled is the dissipation term ε. This term is the most difficult to model because the majority of dissipation occurs at high wave numbers. In LES, these scales are poorly resolved or completely unresolved, making it difficult to estimate. Unfortunately, an accurate estimate of the dissipation is critical because the dissipation and production terms are typically the largest terms in the subgrid kinetic energy equation. In the following paragraphs, several alternative methods of modeling dissipation are discussed.

A natural approach to model the dissipation might be a dynamic model. An analogous Leonard-type dissipation term is defined by

$$L_\varepsilon = \nu\left(\overline{\frac{\partial u_i}{\partial x_j}}\frac{\partial \overline{u_i}}{\partial x_j} - \frac{\partial \overline{u_i}}{\partial x_j}\frac{\partial \overline{u_i}}{\partial x_j}\right) = \varepsilon_t - \hat{\varepsilon} \tag{63}$$

where ε and ε_t are the dissipations at the grid and test level, respectively. Note that by using the Cauchy–Schwarz inequality it is easy to show that L_ε is always positive. The Leonard-type term for dissipation is useful because it exactly gives the difference in dissipation

at the two filter levels. Replacing the dissipations with models and adding a dynamic coefficient gives

$$L_\varepsilon = C\varepsilon_{t\_\text{model}} - \cancel{C}\varepsilon_{\text{model}} \tag{64}$$

Unfortunately, a dissipation model that scales well at both filter levels could not be found, and, therefore, this approach could not used.

A second approach to modeling the dissipation would be to add an additional transport equation for subgrid dissipation. The incompressible subgrid dissipation equation is given by

$$\frac{\partial \varepsilon}{\partial t} + \overline{u}_j \frac{\overline{\partial \varepsilon}}{\partial x_j} + \tau_{u_i u_k u_i} = -\frac{\partial \tau_{u_i P}}{\partial x_i} + \nu \frac{\partial^2 \varepsilon}{\partial x_j \partial x_j} - \varepsilon_d + 2\nu \frac{\partial \overline{u}_i}{\partial x_j} \frac{\partial}{\partial x_j} \frac{\partial \tau_{ik}}{\partial x_k} - \frac{\partial \tau_{u_i \varepsilon}}{\partial x_k} \tag{65}$$

where

$$\tau_{u_i u_k u_i} = 2\nu \left(\overline{\frac{\partial u_i}{\partial x_j} \frac{\partial u_k}{\partial x_j} \frac{\partial u_i}{\partial x_k}} - \frac{\partial \overline{u}_i}{\partial x_j} \frac{\partial \overline{u}_k}{\partial x_j} \frac{\partial \overline{u}_i}{\partial x_k} \right) \tag{66}$$

$$\tau_{u_i P} = 2\nu \left[\frac{\partial}{\partial x_i} \left(\overline{\frac{\partial u_i}{\partial x_j} \frac{\partial P}{\partial x_j}} \right) - \frac{\partial}{\partial x_i} \left(\frac{\partial \overline{u}_i}{\partial x_j} \frac{\partial \bar{P}}{\partial x_j} \right) \right] \tag{67}$$

$$\varepsilon_d = 2\nu^2 \left(\overline{\frac{\partial^2 u_i}{\partial x_k \partial x_j} \frac{\partial^2 u_i}{\partial x_k \partial x_j}} - \frac{\partial^2 \overline{u}_i}{\partial x_k \partial x_j} \frac{\partial^2 \overline{u}_i}{\partial x_k \partial x_j} \right) \tag{68}$$

$$\tau_{u_k \varepsilon} = \nu \left[\overline{\left(u_k \frac{\partial u_i}{\partial x_j} \frac{\partial u_i}{\partial x_j} \right)} - \overline{u}_k \overline{\left(\frac{\partial u_i}{\partial x_j} \frac{\partial u_i}{\partial x_j} \right)} \right] \tag{69}$$

The difficulty of adding a transport equation for dissipation is that four additional unclosed terms are added. For this reason, this approach was not taken. However, it is believed that an accurately modeled dissipation transport equation could significantly improve the dynamic structure model.

A third approach might be to directly model the dissipation using the series expansion (58). A model of this type would take the form

$$\varepsilon = \nu(2\alpha) \frac{\partial^2 \overline{u}_i}{\partial x_j \partial x_k} \frac{\partial^2 \overline{u}_i}{\partial x_j \partial x_k} + \nu \frac{1}{2!} (2\alpha)^2 \frac{\partial^3 \overline{u}_i}{\partial x_j \partial x_k \partial x_l} \frac{\partial^3 \overline{u}_i}{\partial x_j \partial x_k \partial x_l} + \cdots \tag{70}$$

The problem with this approach is that, as stated, for fully developed turbulence the majority of the dissipation occurs at the high wave numbers. This property requires keeping many terms in the series to predict accurately the dissipation. This is not desirable because the higher-order derivatives are computationally expensive to evaluate accurately. An additional issue is that this model does not respond to the subgrid kinetic energy. In other words, the dissipation may be large where there is relatively little subgrid kinetic energy, or it may be small where there is a relatively large amount of subgrid kinetic energy. For these reasons, a model of this type was not used.

The final approach that was used to develop a model for the dissipation was to make it a function of the subgrid kinetic energy k. Expanding the subgrid kinetic energy in its infinite series form gives

$$2k = 2\alpha \frac{\partial \overline{u}_i}{\partial x_j} \frac{\partial \overline{u}_i}{\partial x_j} + \frac{1}{2!} (2\alpha)^2 \frac{\partial^2 \overline{u}_i}{\partial x_j \partial x_k} \frac{\partial^2 \overline{u}_i}{\partial x_j \partial x_k} + \frac{1}{3!} (2\alpha)^3 \frac{\partial^3 \overline{u}_i}{\partial x_j \partial x_k \partial x_l} \frac{\partial^3 \overline{u}_i}{\partial x_j \partial x_k \partial x_l} + \cdots \tag{71}$$

As an aside, Eq. (71) can also be used to initialize the subgrid kinetic energy field. Rearranging Eq. (71) to match the form of the dissipation equation (70) gives

$$\frac{2!}{(2\alpha)} \left(2k - 2\alpha \frac{\partial \overline{u}_i}{\partial x_j} \frac{\partial \overline{u}_i}{\partial x_j} \right) = (2\alpha) \frac{\partial^2 \overline{u}_i}{\partial x_j \partial x_k} \frac{\partial^2 \overline{u}_i}{\partial x_j \partial x_k} + \frac{2!}{3!} (2\alpha)^2 \frac{\partial^3 \overline{u}_i}{\partial x_j \partial x_k \partial x_l} \frac{\partial^3 \overline{u}_i}{\partial x_j \partial x_k \partial x_l} + \cdots \tag{72}$$

where we divided by α by assuming that the computational grid is uniformly spaced ($\mathrm{d}x = \mathrm{d}y = \mathrm{d}z$). Comparing Eq. (72) to (70) reveals that the first term in the series of Eq. (72) is the same as the first term of Eq. (70) except for the viscosity coefficient. The remaining terms in the series (72) are smaller than the terms in the dissipation series (70). Nevertheless, a reasonable model for dissipation is

$$\varepsilon \cong \nu \frac{2!}{(2\alpha)} \left(2k - 2\alpha \frac{\partial \overline{u}_i}{\partial x_j} \frac{\partial \overline{u}_i}{\partial x_j} \right) \tag{73}$$

Note that, with reference to Eq. (72), it is clear that, for an accurate estimate of the subgrid kinetic energy, the dissipation predicted by Eq. (73) must be positive. The series also indicates that the dissipation will be underpredicted. The first term in the dissipation model series (72) is identical to the first term in the exact series (70); however, the series underpredicts each of the higher-order terms when compared to the exact series. In practice, the model for dissipation tends to stay positive except at relatively high Reynolds numbers. Thus, for these reasons the model is not acceptable.

To correct for the difficulties in using Eq. (73) directly and to account for the dissipation at the smaller scales, it is useful to look at a series that is similar to the actual dissipation series. The expansion of the Leonard-type term for dissipation can be written as

$$L_\varepsilon = \nu \left(\overline{\frac{\partial \overline{u}_i}{\partial x_j} \frac{\partial \overline{u}_i}{\partial x_j}} - \frac{\partial \overline{u}_i}{\partial x_j} \frac{\partial \overline{u}_i}{\partial x_j} \right) = \nu(2\alpha) \frac{\partial^2 \overline{u}_i}{\partial x_j \partial x_k} \frac{\partial^2 \overline{u}_i}{\partial x_j \partial x_k} + \nu \frac{1}{2!} (2\alpha)^2 \frac{\partial^3 \overline{u}_i}{\partial x_j \partial x_k \partial x_l} \frac{\partial^3 \overline{u}_i}{\partial x_j \partial x_k \partial x_l} + \cdots \tag{74}$$

The Leonard-type term L_ε can be calculated exactly from the resolved field. Note that the test filtering operation in Eq. (74) has been replaced with a second grid level filtering operation. This form was found to be more accurate for the dissipation model developed hereafter. Subtracting the first term in the series (74) from both sides gives

$$L_\varepsilon - \nu(2\alpha) \frac{\partial^2 \overline{u}_i}{\partial x_j \partial x_k} \frac{\partial^2 \overline{u}_i}{\partial x_j \partial x_k} = \nu \frac{1}{2!} (2\alpha)^2 \frac{\partial^3 \overline{u}_i}{\partial x_j \partial x_k \partial x_l} \frac{\partial^3 \overline{u}_i}{\partial x_j \partial x_k \partial x_l} + \cdots \tag{75}$$

The left-hand side of Eq. (75) gives an estimation of the truncation error of the twice-filtered field. This expression is used to estimate the truncation error in Eq. (73). Normalizing Eq. (75) by the first term of the series gives a ratio of the relative magnitudes of the first term in the series compared to the remaining terms. This ratio can now be used to correct the model for dissipation (73). The new model for dissipation is now

$$\varepsilon \cong \left[\nu \frac{2!}{(2\alpha)} \left(2k - 2\alpha \frac{\partial \overline{u}_i}{\partial x_j} \frac{\partial \overline{u}_i}{\partial x_j} \right) \right] + C_\varepsilon \left[\nu \frac{2!}{(2\alpha)} \left(2k - 2\alpha \frac{\partial \overline{u}_i}{\partial x_j} \frac{\partial \overline{u}_i}{\partial x_j} \right) \right] \times \left(L_\varepsilon - \nu(2\alpha) \frac{\partial^2 \overline{u}_i}{\partial x_j \partial x_k} \frac{\partial^2 \overline{u}_i}{\partial x_j \partial x_k} \right) \Bigg/ \left(\nu(2\alpha) \frac{\partial^2 \overline{u}_i}{\partial x_j \partial x_k} \frac{\partial^2 \overline{u}_i}{\partial x_j \partial x_k} \right) \tag{76}$$

where C_ε is a model constant that is set to 0.667 based on results presented hereafter. With this final form for the dissipation term, a complete model for the subgrid kinetic energy transport equation has now been formulated.

Note that, unlike typical dissipation models, the preceding model contains the molecular viscosity as a coefficient. Here, an attempt has been made to approximate the actual dissipation with a model formulated from the series expansions for dissipation. Although the dissipation model is functional, it is far from ideal for three reasons. First, for a poor estimate of subgrid kinetic energy, the dissipation may become negative (in which case dissipation may be clipped).

Second, to derive the model, a uniform grid was assumed. Last, a model constant must be set. For these reasons, work is continuing on developing a better dissipation model. However, as will be shown later in the paper, for the test case considered, the dissipation model performs adequately.

Even though a complete model has been formulated, the issues of filter size and shape have not been addressed. These issues are critical to obtaining good results because an inappropriate filter size used to determine α will give poor results. In addition, the correct filter size and shape are important for comparing LES results to DNS results. Note that the first filter that is, the grid filter implied by the test filter can be any size. The common choice of selecting the filter size equal to the grid size is completely arbitrary and may not be the best choice.

Three different filter shapes are examined herein: a box filter, a triangle filter, and a Gaussian filter. To determine an acceptable filter size and shape, it is easiest to view them in wave space. We consider a case of a periodic domain of 2π with 64 grid points. Figures 8–10 show the Fourier transform of the Gaussian, box, and triangle filter for this case with three different filter sizes, $\Delta = 1$, 2, and 4. Any wave number greater than 32 cannot be reasonably resolved, and, therefore, it is crucial that the filter completely damp wave numbers greater than 32. Figures 8–10 show that if the first filter is chosen equal to the grid size, the filters do not significantly dampen the higher wave numbers. In our experience, filters of approximately two to four times the grid resolution are appropriate and are used to determine the α factor in the dissipation model (76) and for comparing LES results to DNS results.

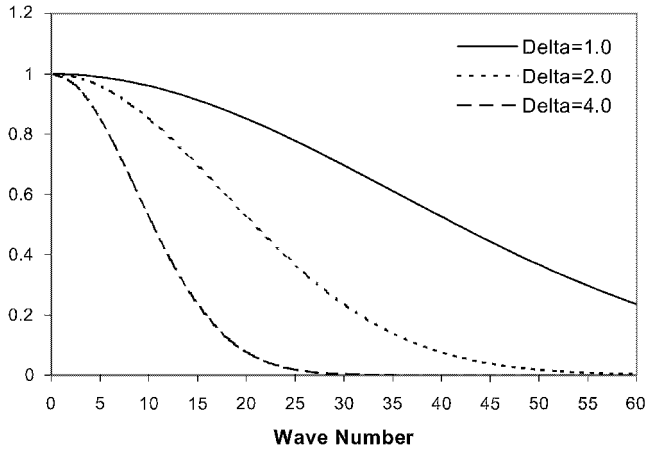

Fig. 8 Gaussian filter in wave space.

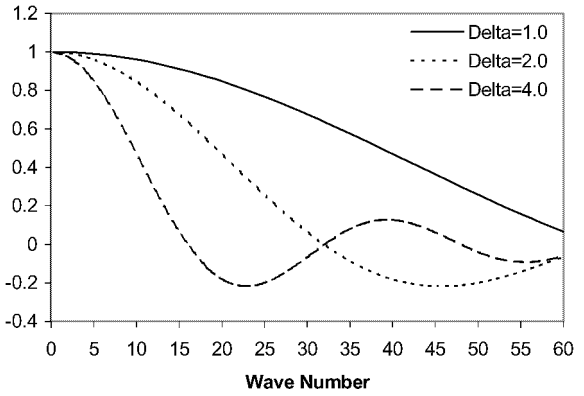

Fig. 9 Box filter in wave space.

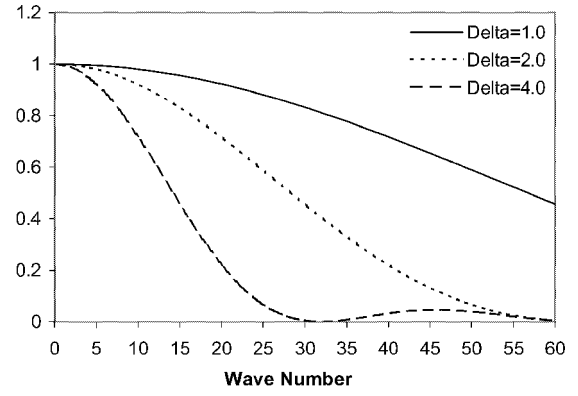

Fig. 10 Triangle filter in wave space.

An appropriate filter shape is more difficult to determine. In dynamic modeling, the first filter and the second filter shapes (here, the second filter function G_2 is defined by $G * \widehat{G}$) are not explicitly specified; only the test filter shape is specified. However, the first filter is related to the test filter by the following expression[26]:

$$G = \widehat{G}(\widehat{\Delta}/\delta) * \widehat{G}(\widehat{\Delta}/\delta^2) * \cdots * \widehat{G}(\widehat{\Delta}/\delta^{\infty}) \qquad (77)$$

where δ is the ratio of the second filter width Δ_2 to the first filter width Δ and the asterisk indicates the convolution operation. Unfortunately, the evaluation of Eq. (77) is an iterative procedure that requires an infinite number of convolution operations per iteration. However, to eliminate the iterations, one can assume that Δ_2 is the same size as $\widehat{\Delta}$. This is not correct but is done here so that the analysis can proceed. When Δ is set equal to four times the grid size and $\widehat{\Delta}$ is set equal to six times the grid size, G can be estimated from a truncated convolution expression. This is done for both the box and the triangle test filter. These filters are shown in Figs. 11 and 12, where it is clear that the first filter calculated from the convolution expression damps the higher wave numbers better than the box or triangle filter of comparable size. In fact, both filters determined from the convolution expression are very similar in shape and appear to be somewhat Gaussian. The primary difference is that the first filter determined from the box test filter is slightly negative

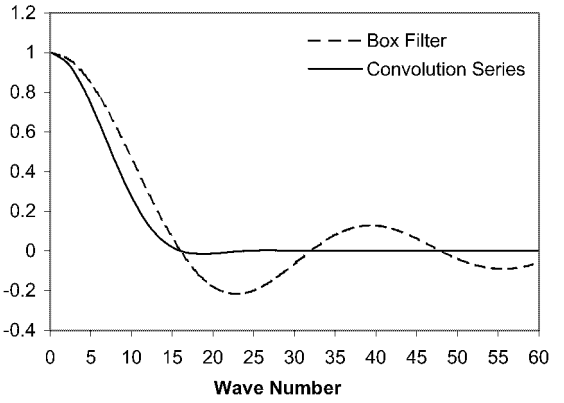

Fig. 11 Box filter given by the first term of Eq. (77); convolution filter given by Eq. (77).

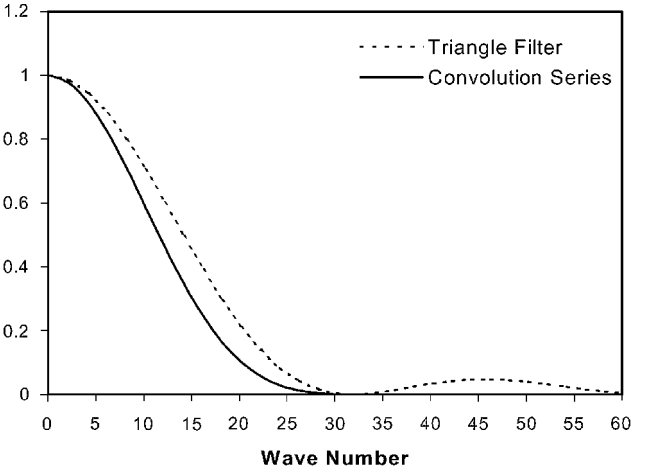

Fig. 12 Triangle filter given by the first term of Eq. (77); convolution filter given by Eq. (77).

in wave space at a wave number of 15; this is not the case for the triangle filter. Despite this difference, it is apparent that the shape of the test filter is not critical to the properties of the grid filter in wave space. The grid filter, calculated in this manner, has significantly better properties in wave space than the parent test box or triangle filter.

VII. Model Test and Results

The only testing shown earlier of the nonviscosity model was to compare the model predicted subgrid stress tensor to the filtered DNS subgrid stress tensor. Although this test is significant, a more complete test should consider the model capability for predicting a time evolving flow. Thus, to validate the one-equation nonviscosity model further, a comparison of the model is made to a DNS simulation of decaying isotropic turbulence.

The DNS validation case was simulated using a pseudospectral code.[17] The Taylor scale Reynolds number ranged from approximately 1000 initially to approximately 60 at the end of the simulation. A three-dimensional periodic box with a domain size of 2π is considered with a grid resolution of 192^3. The initial energy spectrum is shown in Fig. 13. Note that this simulation is much larger than the DNS case used earlier to check the integral equation solvability of different LES models.

The LES simulations use a finite difference nondissipative code that is eighth-order accurate in space and third-order accurate in time.[27] For the LES case, the grid resolution is 64^3. The grid level filter is four times the grid spacing and the test filter, which is a triangle filter, is six times the grid spacing. The LES filtered velocity field is initialized by filtering the DNS field appropriately, whereas the initial subgrid kinetic energy field is determined from Eq. (71).

Because it is expensive to solve Fredholm integral equations, for this simulation the algebraic form of the model is used where the tensor coefficient c_{ij} is removed from the integral. This cannot be strictly justified because the tensor coefficient is a function of space. The effect of removing the coefficient from the integral can be seen from the contour plots of the coefficients for both the integral and algebraic form of the model (Fig. 14). For both cases, the large structures are very similar, with more detail in the algebraic form of the model. The effect of leaving the coefficient inside of the integral is, of course, to smooth the coefficient field. This can also be clearly seen in Fig. 15, where the PDF of the coefficients for both a diagonal and off-diagonal term are shown. Note that, because of the improvements made in the formulation of the model, it is not as critical to leave the coefficients inside of the integral, that is, the coefficients are not as strong a function of space as in other models. In particular, the model formulation is such that the diagonal terms of the tensor coefficients must sum to two, and each term must be positive; for most LES models, there is no restriction on the magnitude of the coefficient.

To compare the LES model to the DNS case, a grid level filter shape must be specified. As discussed earlier, the grid level filter shape is never explicitly specified in an LES simulation. Even though

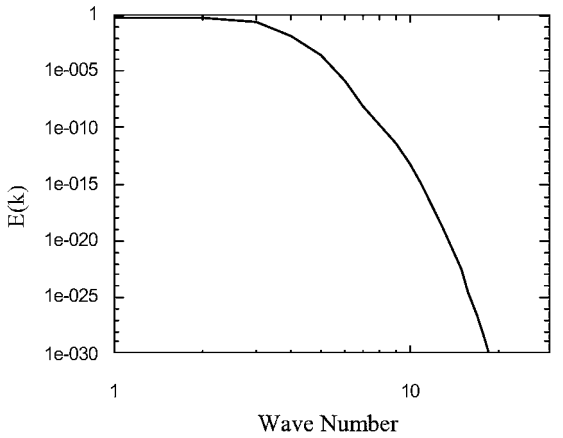

Fig. 13 Initial energy spectrum for the large validation DNS simulation; the maximum energy is at a wave number of 2.0.

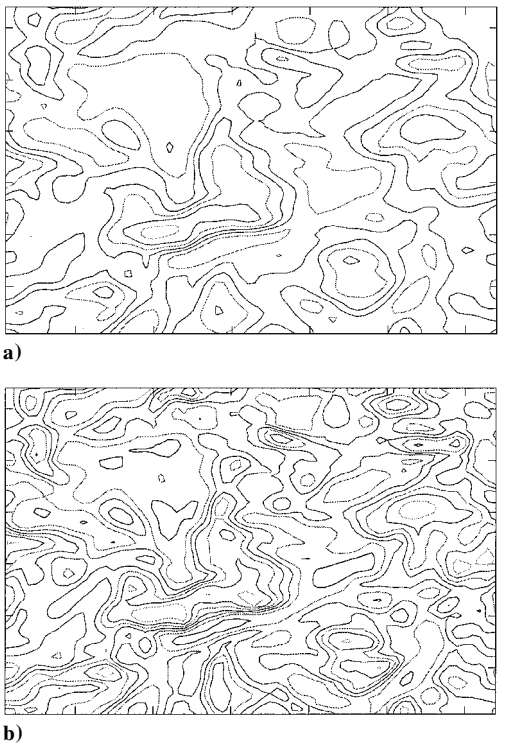

Fig. 14 Contour plot of tensor coefficient (c_{11}) at time 3 s; contours are evenly distributed from 0.2 to 1.6 in both plots: a) coefficients left inside of integral (integral form of the model) and b) coefficients removed from integral (algebraic form of the model).

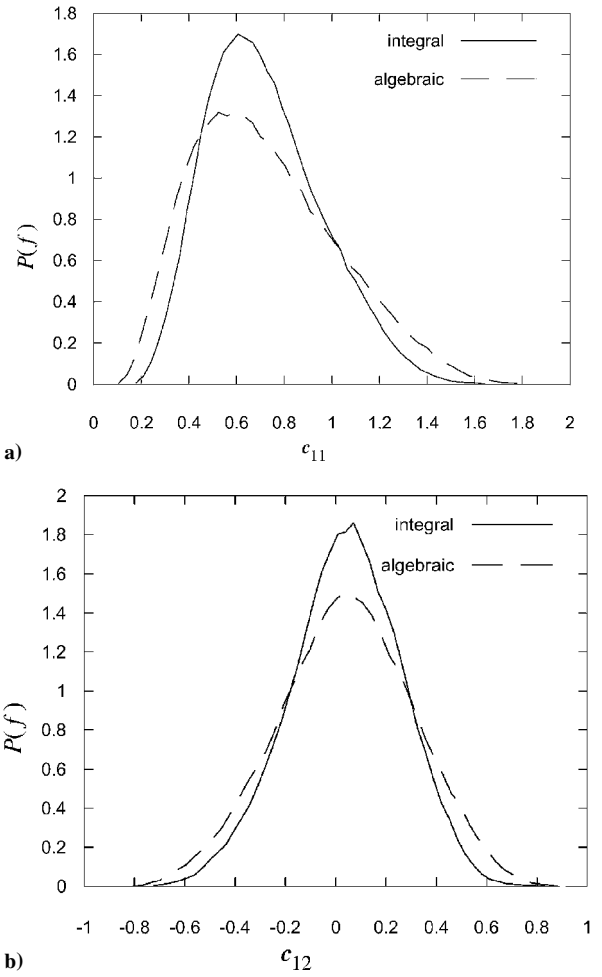

Fig. 15 PDF of the tensor coefficient at time 3 s for a) diagonal term c_{11} and b) off-diagonal term c_{12}.

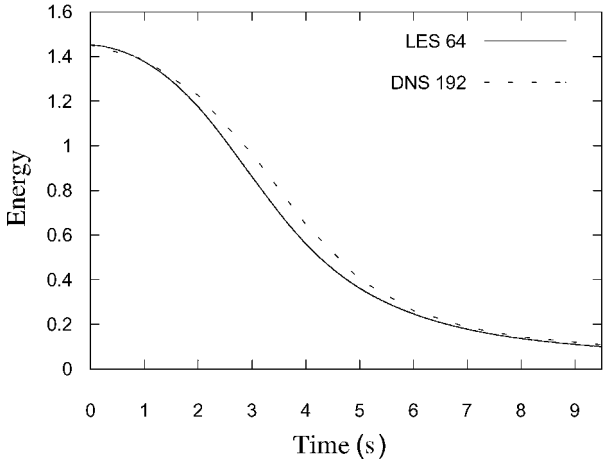

Fig. 16 Comparison of LES calculated resolved energy $\overline{u_i u_i}$ to the filtered DNS calculated energy.

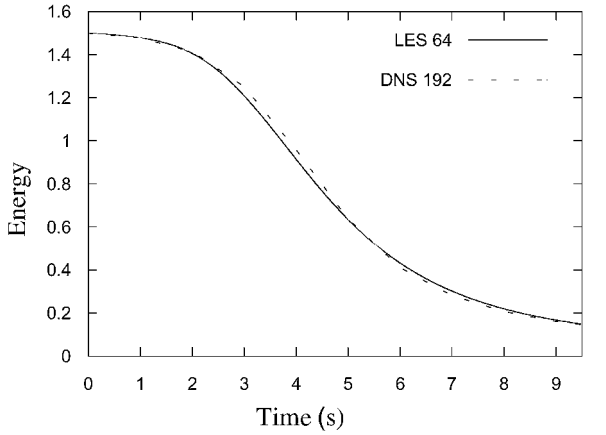

Fig. 17 Comparison of LES calculated total energy $2k + \overline{u_i u_i}$ to the DNS calculated energy $u_i u_i$.

it is not strictly correct, the grid level filter is assumed to also be a triangle. This is done to simplify the numerical calculations. When Fig. 12 is examined, it is clear that the actual grid filter, determined from the convolution expression (77), is similar to the triangle filter; however, the actual grid filter will remove slightly more energy from the resolved field than a triangle filter.

Figure 16 shows a plot of the resolved energy from the LES model and the resolved energy calculated by filtering the DNS field. As expected, the predicted resolved LES energy field is slightly less than the filtered DNS field. This is because the grid filter used to calculate the filtered DNS field energy is approximated by a triangle filter. Nevertheless, there is good agreement between the two fields. Twice the total energy $u_i u_i$ in a LES simulation can be approximated by adding twice the subgrid energy to the resolved energy. In Fig. 17, a comparison of the total LES energy is made to the DNS energy field. In this case, there is also good agreement.

To gain insight into the one-equation nonviscosity model, it is useful to view the resolved energy spectrum in wave space. Ideally, the energy at the low wave numbers will be unaffected by the LES model, and the energy at the higher wave numbers will be reduced or truncated. Figure 18 compares the energy spectrum of the LES simulation to an underresolved (no model) simulation and to a DNS simulation. As can be seen, in the LES simulation, the energy at the higher wave numbers is significantly reduced, whereas the energy at the lower wave numbers is largely unaffected by the model. In contrast, for the underresolved case, a significant amount of energy is piling up at the higher wave numbers.

To verify that the subgrid scale model is significantly affecting the resolved field, a comparison is made, in Fig. 19, of the LES resolved field to the underresolved case. As expected, the LES predicted resolved energy is significantly less than the underresolved case.

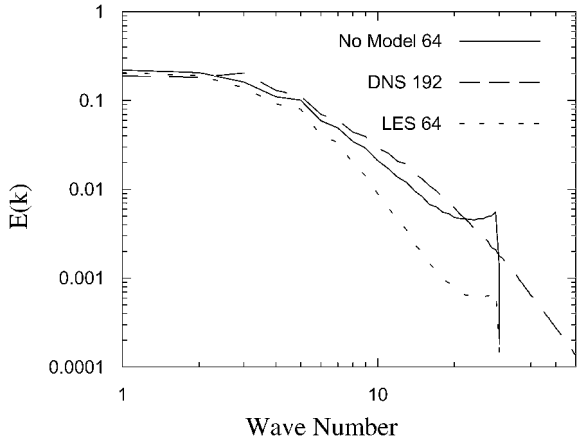

Fig. 18 Energy spectrums in wave space at a simulation time of 3 s; three cases are shown: an underresolved case (no model), a DNS case, and an LES case.

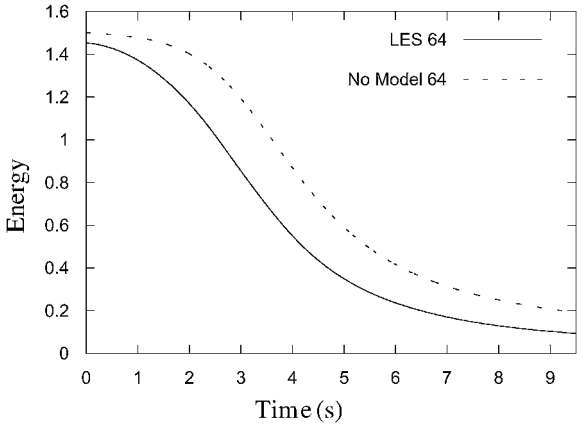

Fig. 19 Comparison of LES resolved energy $\overline{u_i u_i}$ to the energy of an underresolved simulation (no model) 64^3 grid points.

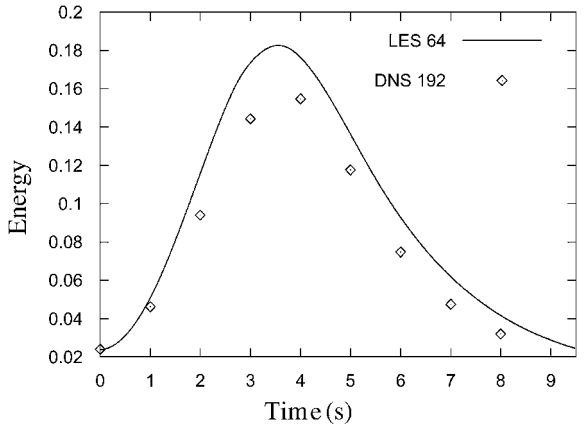

Fig. 20 Comparison of LES calculated subgrid kinetic energy to the filtered DNS subgrid kinetic energy.

The lower energy level in the LES simulation is due to the reduction of energy at the higher wave numbers, as shown in Fig. 18.

Because the subgrid kinetic energy is the scaling term for the one-equation nonviscosity model, it is critical that the LES model accurately predicts the subgrid kinetic energy. Figure 20 shows a plot of the LES calculated subgrid kinetic energy compared to the filtered DNS subgrid kinetic energy. As can be seen, there is good agreement. This plot also indicates that the production and dissipation models are performing adequately and that they are properly balanced. Shown in Fig. 21 is a plot of the subgrid dissipation ε and subgrid production, $\tau_{ij}\overline{S}_{ij}$, terms in the subgrid kinetic energy transport equation. The subgrid production and the subgrid dissipation

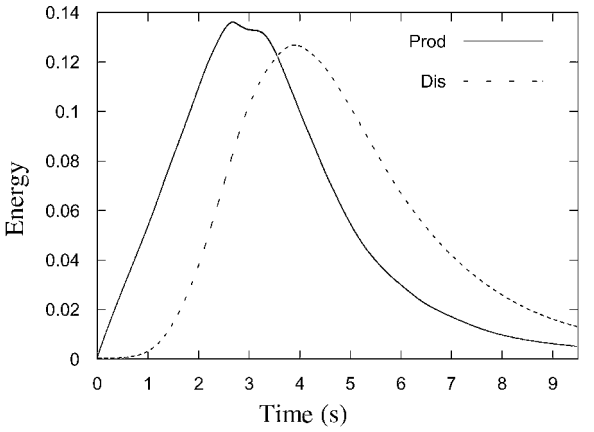

Fig. 21 LES subgrid dissipation ε and production $\tau_{ij}\,\overline{S_{ij}}$ as a function of time.

perform as expected. Initially, when all of the energy is at the large scales (see Fig. 18) energy is cascading to the smaller scales, and, therefore, production of subgrid kinetic energy is increasing. Later in the simulation, when the subgrid kinetic energy is large (indicating more energy at small scales) the dissipation increases appropriately. Finally, toward the end of the simulation, when little energy is left, both the subgrid dissipation and subgrid production decay. Note that these values are averaged over the entire domain. Locally, production may be negative (accounting for backscatter), but, when averaged over the entire domain, subgrid production is always positive.

VIII. Conclusions

A new dynamic one-equation nonviscosity LES model or dynamic structure model has been introduced. The new model estimates the actual subgrid stress tensor using the dynamic methodology to obtain a tensor coefficient and from a transport equation for the subgrid kinetic energy. The nonviscosity model formulation removes the problems and mathematical inconstancies associated with common LES viscosity subgrid models, especially those based on the resolved scale strain rate.

Integral equations are fundamental to the dynamic approach. The integral equations that result from the one-equation nonviscosity model have been shown to be solvable; this is not the case for the dynamic Smagorinsky model (see Ref. 1) and the dynamic one-equation model of Ghosal et al.[13] Even though most formulations remove the dynamic coefficient from the integral and avoid solvability issues, we believe the underlying solvability of all dynamic models should be addressed to avoid potential inconsistencies.

It has been shown that the conventional dynamic models do not scale well with the filter level. This poor scaling is one factor that leads to a poor estimate of the actual subgrid stress tensor. The new one-equation nonviscosity model has been shown to scale much better than conventional models because it relies on the subgrid turbulent kinetic energy for scaling. The improved scaling leads to a significantly better estimate of the actual subgrid stress tensor.

In the case of decaying isotropic turbulence, the new dynamic structure model has been shown to compare well with DNS results. The model correctly predicts the proper amount of both the resolved and the subgrid kinetic energy at all times. Finally, we note that the new model and its general approach could be extended to scalar transport modeling.

Acknowledgments

This material is based on work supported by the U.S. Army Research Office under Grant DAAH04-94-G-0328. We would like to thank Leslie Smith, Rolf Reitz, Fritz Bedford, Sergei Chumakov, Daniel Lee, and Scott Mason for valuable discussions and the Engine Research Center and Silicon Graphics, Inc.-Cray Research for providing computing facilities.

References

[1]Germano, M., Piomelli, U., Moin, P., and Cabot, W. H., "A Dynamic Sub-Grid-Scale Eddy Viscosity Model," *Physics of Fluids*, Vol. 3, No. 7, 1991, pp. 1760–1765.

[2]Menon, S., Yeung, P. K., and Kim, W. W., "Effect of Subgrid Models on the Computed Interscale Energy Transfer in Isotropic Turbulence," *Computers and Fluids*, Vol. 25, No. 2, 1996, pp. 165–180.

[3]Speziale, C. G., "Turbulence Modeling for Time-Dependent RANS and VLES: A Review," *AIAA Journal*, Vol. 36, No. 2, 1998, pp. 173–184.

[4]Ghosal, S., and Moin, P., "The Basic Equations for the Large Eddy Simulation of Turbulent Flows in Complex Geometry," *Journal of Computational Physics*, Vol. 118, No. 1, 1995, pp. 24–37.

[5]Deardorff, J. W., "A Numerical Study of Three-Dimensional Turbulent Channel Flow at Large Reynolds Numbers," *Journal of Fluid Mechanics*, Vol. 41, 1970, pp. 453–480.

[6]Ghosal, S., "An Analysis of Numerical Errors in Large-Eddy Simulations of Turbulence," *Journal of Computational Physics*, Vol. 125, No. 1, 1996, pp. 187–206.

[7]Meneveau, C., "Statistics of Turbulence Subgrid-Scale Stresses: Necessary Conditions and Experimental Tests," *Physics of Fluids*, Vol. 6, No. 2, 1994, pp. 815–833.

[8]Piomelli, U., Cabot, W. H., Moin, P., and Lee, S., "Sub-Grid-Scale Backscatter in Turbulent and Transitional Flows," *Physics of Fluids*, Vol. 3, No. 7, 1991, pp. 1766–1771.

[9]Langford, J. A., and Moser, R. D., "Optimal LES Formulations for Isotropic Turbulence," *Journal of Fluid Mechanics*, Vol. 398, 1999, pp. 321–346.

[10]Smagorinsky, J., "General Circulation Experiments with the Primitive Equations," *Monthly Weather Review*, Vol. 93, 1963, pp. 99–165.

[11]Jiménez, J., and Moser, R. D., "Large-Eddy Simulations: Where Are We and What Can We Expect?," *AIAA Journal*, Vol. 38, No. 4, 2000, pp. 605–612.

[12]Akselvoll, K., and Moin, P., "Large Eddy Simulation of Turbulent Confined Coannular Jets and Flow Over a Backward Facing Step," Thermosciences Div., Dept. of Mechanical Engineering, Rept. TF-63, Stanford Univ., Stanford, CA, 1995.

[13]Ghosal, S., Lund, T. S., Moin, P., and Akselvoll, K., "A Dynamic Localization Model for Large-Eddy Simulation of Turbulent Flows," *Journal of Fluid Mechanics*, Vol. 286, 1995, pp. 229–255.

[14]Lilly, D. K., "A Proposed Modification of the Germano Sub-Grid-Scale Closure Method," *Physics of Fluids*, Vol. 4, No. 3, 1992, pp. 633–635.

[15]Meneveau, C., Lund, T. S., and Cabot, W. H., "A Lagrangian Dynamic Sub-Grid-Scale Model of Turbulence," *Journal of Fluid Mechanics*, Vol. 319, 1996, pp. 353–385.

[16]Schumann, U., "Realizability of the Reynolds-Stress Turbulence Models," *Physics of Fluids*, Vol. 20, No. 5, 1977, pp. 721–725.

[17]Rogallo, R. S., "Numerical Experiments in Homogeneous Turbulence," NASA TM 81315, 1981.

[18]Kanwal, R. P., *Linear Integral Equations*, Academic Press, New York, 1971, pp. 1–60.

[19]Hochstadt, H., *Integral Equations*, Wiley, New York, 1973, pp. 1–24.

[20]Pomraning, E., "Development of Large Eddy Simulation Turbulence Models," Ph.D. Dissertation, Mechanical Engineering Dept., Univ. of Wisconsin, Madison, WI, 2000.

[21]Bardina, J., Ferziger, J. H., and Reynolds, W. C., "Improved Subgrid Scale Models for Large-Eddy Simulation," AIAA Paper 80-1357, 1980.

[22]Meneveau, C., and Katz, J., "Scale-Invariance and Turbulence Models for Large-Eddy Simulation," *Annual Review of Fluid Mechanics*, Vol. 32, 2000, pp. 1–37.

[23]Liu, S., Meneveau, C., and Katz, J., "On the Properties of Similarity Subgrid-Scale Models as Deduced from Measurements in a Turbulent Jet," *Journal of Fluid Mechanics*, Vol. 275, 1994, pp. 83–119.

[24]Ghosal, S., "Mathematical and Physical Contraints on LES," AIAA Paper 98-2803, 1998.

[25]Bedford, K. W., and Yeo, W. K., "Conjuctive Filtering Procedures in Surface Water Flow and Transport," *Large Eddy Simulation of Complex Engineering and Geophysical Flows*, edited by B. Galperin, and S. A. Orszag, Cambridge Univ. Press, New York, 1993, pp. 513–539.

[26]Carati, D., and Vanden Eijnden, E., "On the Self-Similarity Assumption in Dynamic Models for Large Eddy Simulation," *Physics of Fluids*, Vol. 9, No. 7, 1997, pp. 2165–2167.

[27]Mason, S. D., "Direct Numerical Simulations of Turbulent Reacting Shear Layers," Ph.D. Dissertation, Mechanical Engineering Dept., Univ. of Wisconsin, Madison, WI, 2000.

J. R. Bellan
Associate Editor